

# Sliding Behavior of Friction Material Against Cermet Coatings: Pin-on-Disc Study of the Running-in Stage

Matteo Federici,<sup>a</sup> Guido Perricone,<sup>b</sup> Stefano Gialanella,<sup>a</sup> Giovanni Straffelini<sup>a\*</sup>

<sup>a</sup> Dept. of Industrial Engineering, University of Trento, Via Sommarive 9, Povo, Trento, Italy

<sup>b</sup> Brembo SpA, Stezzano, Italy

\* Corresponding Author

**Abstract** Running-in is the initial stage during which a tribological system reaches a steady state condition. In this study, the running-in behavior of a commercial brake friction material, pin-on-disc tested under dry sliding conditions has been investigated to understand the role of different surface finishing of hard coatings. These coatings were deposited onto the cast iron counterface disc and then mechanically polished to achieve set values of average roughness,  $R_a$ , and roughness skewness,  $R_{sk}$ . The tribological data were modeled using an exponential relation for the wear rate, according to a literature approach. The model parameters were related to the above disc surface roughness parameters. The results were interpreted in terms of the main wear mechanisms, that determine the formation of the friction layers on the pins as well as discs wear tracks. Of particular relevance is the finding that a negatively-skewed surface roughness is fundamental to achieve the best running-in performances. The beneficial effects coming from this surface treatment derive from the reduction in abrasion and from improved dynamics in the formation of the friction layer, with particular regard to those parts (secondary plateaus) made of compacted wear debris.

**Keywords** Dry sliding - HVOF coatings - Friction material - Running-in - Braking materials

## 1 Introduction

In general, when two flat surfaces start a sliding contact, they undergo a transient process that leads to the increase in their real area of contact. Such increase is due to the progressive wearing out of the two mating bodies. In particular, the sharp asperities of each surface are flattened leading to a smoother and more uniform sliding contact [1]. This phenomenon is known as *running-in* process. As noted by Blau [2], in some cases additional wear processes can play an important role in the running-in stage. For example, the accumulation of wear debris and the related material transfer phenomena from one surface to the other may change the contact conditions, including the chemical and micro-mechanical properties of the friction layers that form at the interface of the mating materials. This situation is particularly important in vehicular braking systems, made of friction linings, involving a pair of brake pads, sliding against a counterface disc [3,4]. In this case, the running-in can be regarded as the period necessary to form a uniform friction layer capable to provide the proper friction coefficient and, thereby, braking torque. The main components of the friction layer are the so-called primary and secondary plateaus [3,4]. Primary plateaus are made of hard and tough constituents, like metallic fibers and/or relatively large ceramic fillers [3-6]. The secondary plateaus are formed by the piling up of wear debris, originating from the wearing out of both the friction material and the counterface disc. These particles are stopped by and pressed against the primary plateaus [7-9]. Generally speaking, the compactness and stability of the friction layers determine the stability of the friction coefficient and also the achievement of an adequately low wear rate [7-9].

Several investigations focused on the study of the evolution of the surface topography during the running-in period and on the prediction of the wear rate of the mating bodies through mathematical models [10-14]. Zheng et al. [14], for example, studied the friction and the wear behavior of a spark-ignited engine during the running-in period by applying the mathematical model proposed by Schneider et al. [15]. Their model, based on the fit of their experimental data, describes a first-order exponential decrease of the wear rate as a function of the sliding time. They noted that the wear rate,  $W$ , went through a maximum at the beginning of the sliding run and then it progressively decreased towards a constant, steady state value ( $W_\infty$ ):

$$W = A_1 e^{-\frac{t}{t_1}} + W_\infty \quad (1)$$

where  $A_1$  is the difference between the wear rate at the beginning of the sliding,  $t=0$ , and the steady state wear rate, being  $t_1$  the time constant of the model.

In a previous study [16], the application of some cermet coatings via the high velocity oxygen fuel (HVOF) process onto the disc surfaces, evidenced the role of the surface roughness and skewness on the frictional and wear performances of a pin-disc system. To the Authors' knowledge the study of the running-in of the disc-pad system has been little investigated in literature so far, especially as concerns this newly-developed coated braking discs. This study, based on pin-on-disc (PoD) tests, aims at investigating the tribological mechanisms active during running-in. Although PoD is not reproducing real braking conditions, it is an excellent tool for verifying preliminarily materials properties in view of their complete assessment in real systems, using specific dyno-tests and bench

tests with full-size discs and real pads and, eventually, car tests conducted according to certified driving cycles.

## 2 Materials and experimental procedures

The sliding tests were carried out using an Eyre/Biceri PoD test rig. The discs had a diameter of 63 mm and were machined from a real gray cast iron braking disc with a pearlitic microstructure [17,18]. After machining the discs were coated with an industrial HVOF deposition apparatus. Two different feedstock composite powders were used. The first one was a commercial WC-CoCr powder with a nominal composition of 86 wt.% WC in a 10 wt.% Co 4 wt.% Cr matrix. The second powder employed in the HVOF deposition, was a commercial Cr<sub>3</sub>C<sub>2</sub>-NiCr powder containing 75 wt.% Cr<sub>3</sub>C<sub>2</sub> particles embedded in a 25 wt.% NiCr matrix. The WC-CoCr powder was produced by agglomeration and sintering while, the Cr<sub>3</sub>C<sub>2</sub>-NiCr one, was obtained by sintering and plasma densification. The average particle-size distribution of the WC-CoCr powder was in the range 10-25 μm. The Cr<sub>3</sub>C<sub>2</sub>-NiCr powder had a higher average particle-size which was between 10-45 μm. Several studies [19-22] confirm the superior room temperature wear-resistance of the WC-CoCr coatings with respect the Cr<sub>3</sub>C<sub>2</sub>-NiCr ones. On the other hand, chromium carbide coatings exhibit better properties at higher temperatures [23,24]. For these reasons, a comparative study on these two coating systems has been carried out, to explore their thermo-mechanical stability under the different contact pressures and temperatures induced by the wear testing conditions.

The spray parameters were extensively studied in previous researches [19,20]. In the present study, typical parameters for the deposition of the cermet coatings via HVOF were adopted. The kerosene and the oxygen flow rates were about 24L/h and 950 L/min and the spray distance was selected at around 380 mm. In order to improve the adhesion and the coating properties, the discs were preheated using a plasma torch.

Coating	Microhardness [HV0.3]	Surface roughness R <sub>a</sub> , μm		Skewness R <sub>sk</sub>	
		As-sprayed	Polished	As-sprayed	Polished
WC-CoCr	1130 ± 90	2.7	1.1	0.2	-1.5
Cr <sub>3</sub> C <sub>2</sub> -NiCr	916 ± 84	4.7	1.0	0.3	-2.3

Table 1: Main characteristics of the HVOF cermet coatings.

The main characteristics of the coatings are summarized in Table 1. The microhardness measurements were made on the coating cross sections using a Vickers indenter under a load of 300 g. The Cr<sub>3</sub>C<sub>2</sub>-NiCr coating is characterized by a lower microhardness, and a higher surface roughness R<sub>a</sub>, determined using a standard stylus profilometer [21,22]. This feature of the coating is compatible with the coarser particle size of the Cr<sub>3</sub>C<sub>2</sub>-NiCr starting powder. Following the indications of a previous investigation [16], it was also decided to submit the coatings to an optimized surface polishing treatment, in order to obtain a surface roughness (R<sub>a</sub>) of around 1 μm.

The polishing procedure is summarized in Table 2.

Disc	Final Roughness $R_a$ [ $\mu\text{m}$ ]	Polishing Procedure
Coating A	1	Diamond disc (220 grit) 30 s
Coating B	1	Diamond disc (220 grit) 15 s

Table 2: Polishing procedure of the coated discs [16].

The skewness parameter ( $R_{sk}$ ), described in the ISO 4287-1997 standard, was calculated by using equation (2). The data are included in Table 1.

$$R_{sk} = \frac{1}{R_q^3} \frac{1}{n} \sum_{i=1}^n (y_i - \bar{y})^3 \quad (2)$$

where  $R_q$  is the root mean square roughness,  $y_i$  is the height of the  $i$ -th point and  $\bar{y}$  is the mean of  $y$ . According to the ISO 4287-1997 standard, if  $R_{sk} = 0$  the surface is symmetrical, as concerns peaks and valleys, with respect to the average line. In this case, the distribution of the heights can be Normal or Gaussian. Furthermore, a positive value of  $R_{sk}$  indicates the prevailing presence of peaks on the surface; while a negative value of  $R_{sk}$  is representative of a larger amount of valleys. In the as-sprayed condition,  $R_{sk}$  is slightly positive in agreement with published data [25-28]. After polishing, it becomes negative, because of the flattening of the highest asperities. As a consequence of this flattening, the load-bearing area of the coated discs increases [16,25-28]. This polishing procedure led to a decrease in the coating thickness from about 70  $\mu\text{m}$  in the as-sprayed conditions to the 50-60  $\mu\text{m}$  after polishing.

As mentioned, the surface parameters were measured by means of a stylus profilometer, the scanned length was equal to 15 mm in the region outside the wear tracks and 6 mm for the measurements within the wear tracks. In order to get rid of systematic errors due to the change in the scanning velocity, it was set equal to 0.15 mm/s for all the measurements. To ensure a statistical relevance five measurements were performed for each condition.

The pins were made of a commercial low-metallic friction material and they were machined from a real brake pad. The friction material was made of several constituents, listed, according to the relevant functional categories [29,30], in Table 3. In Fig. 1 the scanning electron microscopy (SEM) micrograph shows the microstructure of the friction material, with some constituents are identified and labeled by means of energy dispersive X-ray spectroscopy (EDXS) analyses. The pins had cylindrical shapes with a diameter and a height of 6 and 10 mm respectively. The flat end of each pin was in contact with the rotating surface of the coated disc during the entire PoD test. The parallelism of the pin-on-disc arm was checked before and after each test in order to ensure the perpendicularity between the pin and the disc and to avoid errors due to their misalignment.

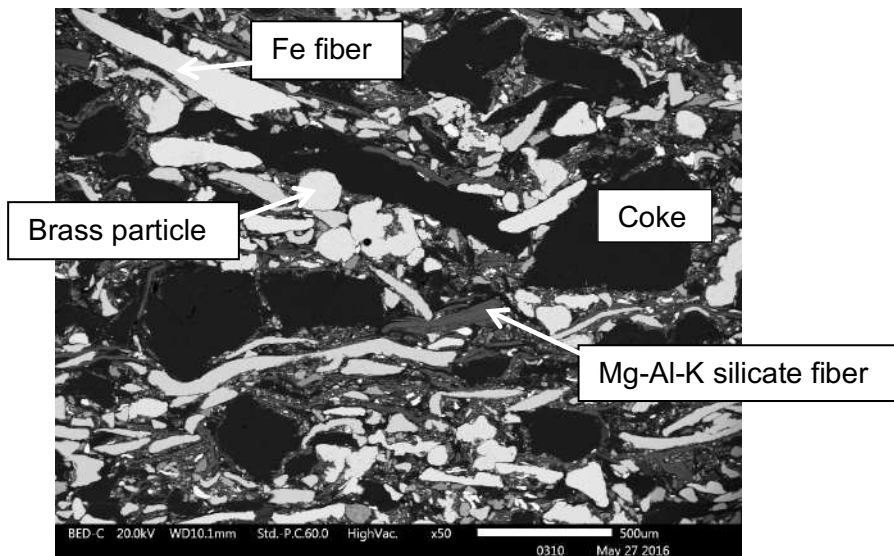


Fig. 1: SEM micrograph of a friction material cross section with the indication of the main constituents.

Group	Volume (%)
Ferrous Metals	7.0
Non-ferrous metals	10.0
Abrasives	12.5
Lubricant	7.0
Fibers	3.5
Fillers	12.0
Carbon	28.6
Phenolic resin	19.4

Table 3: Main components of the low metallic friction material investigated in the present study [30].

The PoD tests were carried out at a sliding velocity of 1.57 m/s and at room temperature. The nominal contact pressure was equal to 1 MPa [6,16,18,31]. In order to evaluate the wear volumes of the pins during the running-in. The tests were interrupted every 2 minutes until the steady-state wear rate was almost reached (*interrupted tests*). The mass loss of the pins was evaluated at each interruption by means of an analytical balance with a precision of  $10^{-4}$  g. The wear volumes,  $V$ , were then calculated by dividing the weight loss by the density of the pins ( $2.8 \text{ g/cm}^3$ ). The wear rates,  $W$ , were calculated as:

$$W = \frac{V}{s} \quad (3)$$

being  $s$  the sliding distance. The specific wear coefficients,  $K_a$ , were also calculated, using the following expression:

$$K_a = \frac{W}{F} \quad (4)$$

where  $F$  is the applied load. The average friction coefficients, evaluated for each time interval, were also continuously recorded during the tests. For the sake of comparison, tests without any stop were also carried out, and correspondingly, the continuous evolution of the friction coefficient was recorded (*continuous tests*). The coatings and the worn out surfaces of the pins were analyzed in a JEOL IT300 scanning electron microscope (SEM) in order to characterize their surface topography and the wear tracks.

### 3 Results

#### 3.1 Wear Behavior

Fig. 2 depicts the recorded evolution of the pin wear volumes as a function of the sliding time, for the discs in the as-sprayed (a) and polished(b) conditions.

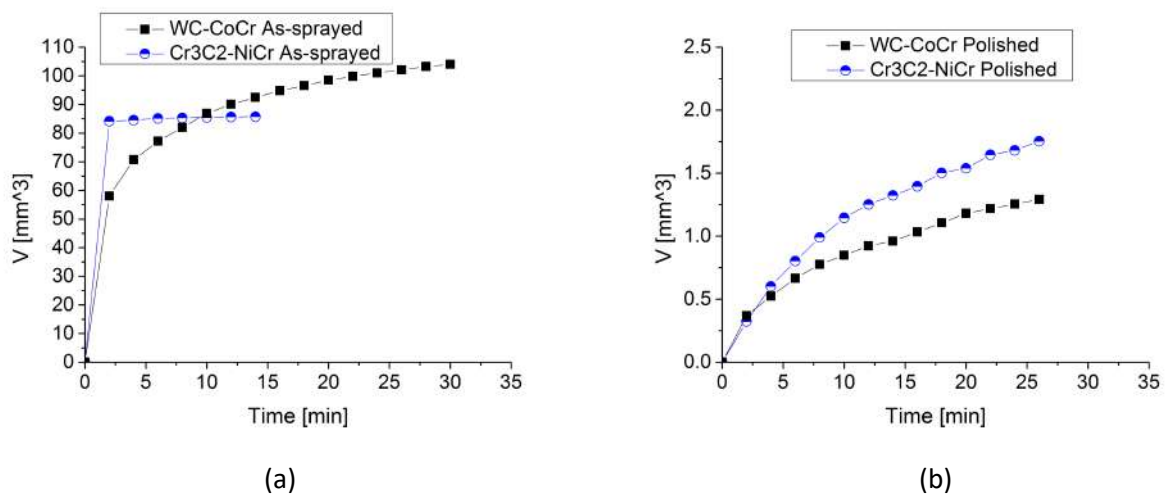


Fig. 2: Wear volume of pins as a function of the sliding time for (a) discs in the as-sprayed conditions and (b) discs with an average roughness of 1 $\mu$ m, obtained by surface polishing. Please note the very different range for the y-axes.

Fig. 2a shows that the initial wear volume for the Cr<sub>3</sub>C<sub>2</sub>-NiCr coating is higher than the one of the WC-CoCr coating. This is related to the difference in the surface roughness in the as-sprayed conditions (Table 1), that is larger for the first coating,  $R_a \approx 5 \mu\text{m}$ , with respect to the second one,  $R_a \approx 3 \mu\text{m}$ . Due to the lower microhardness of the Cr<sub>3</sub>C<sub>2</sub>-NiCr coating, however, the wear volume of the pin after 6 minutes of sliding reaches a steady condition. The higher microhardness of the WC-CoCr coating resulted in a continuous increase in the wear volume of the pin, with a prolonged running-in stage lasting for about 34 minutes. Analyzing the curves in Fig. 2b, referring to surface polished coatings, it is possible to note that both the initial wear volume and the increasing trend of the curves are almost the same for the Cr<sub>3</sub>C<sub>2</sub>-NiCr and WC-CoCr coatings.

The values of the wear volumes were used to calculate the wear rates,  $W$ , whose values are shown in Fig. 3. The experimental points were then fitted using Eq.1. The relevant model parameters are listed in Table 3. First of all, it can be observed that the experimental fit is very good in case of the as-sprayed samples (with adjusted  $R^2$  values very close to unity), whereas in the case of the polished specimens the quality of the fit was lower. This is due to the scatter of results of Fig, 3b, which is most probably due to the difficulties in the weighting operations when dealing with a very little amount of debris. It can be further noted that the steady-state wear rates ( $W_\infty$ ) are always lower for the  $\text{Cr}_3\text{C}_2\text{-NiCr}$  coatings and decrease by one to two orders of magnitude after the polishing treatment.

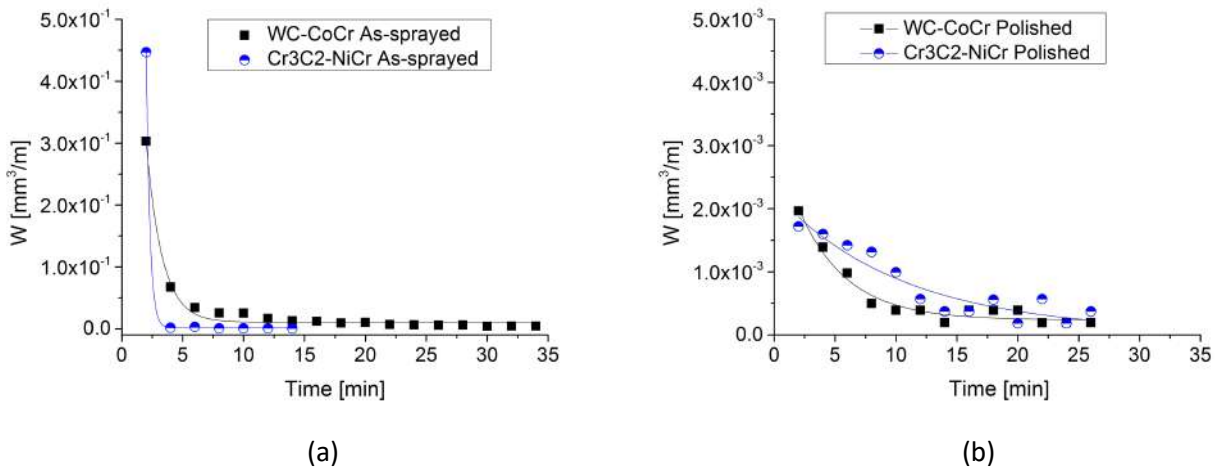


Fig.3: Wear rate of pins as a function of the sliding time for (a) discs in the as-sprayed conditions and (b) discs with an average roughness of 1 $\mu\text{m}$ . Data points are fitted by the continuous lines given by Eq.1 (see main text).

Disc	$A_1$ (mm <sup>3</sup> /m)	$t_1$ (min)	$W_\infty$ (mm <sup>3</sup> /m)	Adj. R-Square
WC-CoCr As sprayed	1.35	1.31	$1.06 \cdot 10^{-2}$	0.99
Cr <sub>3</sub> C <sub>2</sub> -NiCr As sprayed	331.88	0.30	$1.27 \cdot 10^{-3}$	0.99
WC-CoCr Polished	$2.93 \cdot 10^{-3}$	3.96	$2.39 \cdot 10^{-4}$	0.96
Cr <sub>3</sub> C <sub>2</sub> -NiCr Polished	$2.20 \cdot 10^{-3}$	10.40	$5.56 \cdot 10^{-5}$	0.88

Table 4: Fitting parameters of the different curves.

-  $A_1$  is the difference between the wear rate at the beginning of the sliding,  $t=0$ , and the steady state wear rate ( $W_\infty$ );

-  $t_1$  is the time constant of the model.

Since the wear tracks on the coated discs could not be detected with the stylus profilometer, the wear of the discs was assumed to be negligible in comparison to the wear of the pins. The  $W_{\infty}$  values in Table 4 are consistent with the data reported in a previous investigation [31]. As a reference, the steady-state wear rates of the pin and a gray cast iron disc, sliding against each other under the same conditions used in the present study, were equal to  $W_{\infty} = 1.60 \cdot 10^{-3} \text{ mm}^3/\text{m}$  and  $7.8 \cdot 10^{-4} \text{ mm}^3/\text{m}$  respectively. From the values in table 4, it can be concluded that the polished coatings provided a reduction in the overall wear of the pin-disc systems with respect to the uncoated disc condition, investigated in a former study [31].

### 3.2 Frictional behavior

Fig. 4a and 4b show the average friction coefficients, obtained for each time step used for the wear-volume and wear-rate quantifications. For a comparison, Fig. 4c and 4d show the evolution of the friction coefficient in case of the continuous tests.

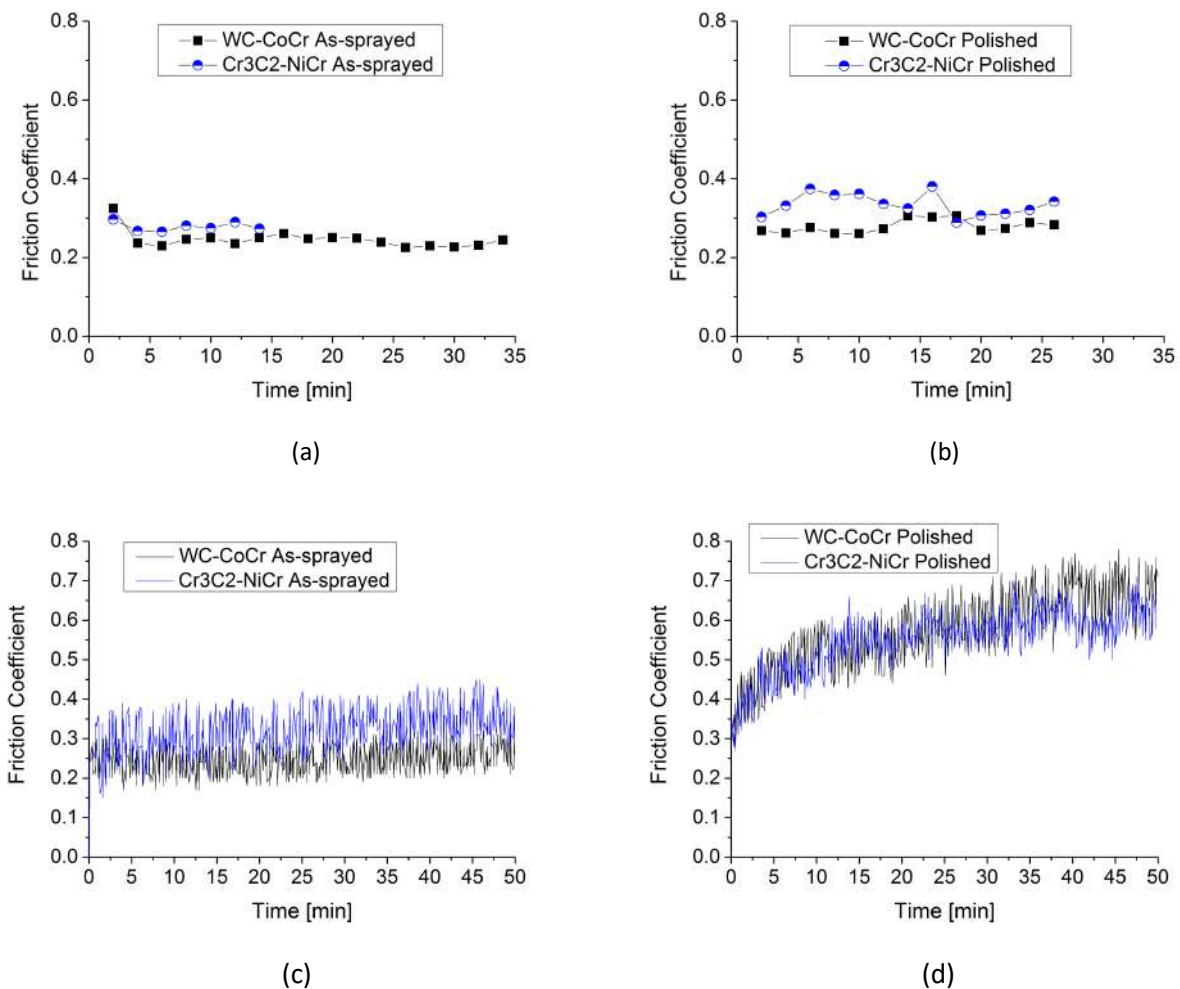


Fig. 4: (a, b) Average friction coefficient in the case of the *interrupted* tests; (c, d): plots of the friction coefficient evolution during the *continuous* tests.



From Fig. 4a and 4b it is possible to note that the friction coefficient for the as-sprayed coatings is on average lower than that for the polished coatings. This aspect is more evident in the continuous wear tests (Fig. 4c and 4d). In these tests the friction coefficient of the as-sprayed coatings is slightly higher than for the interrupted tests on the same samples. For the polished coatings, the friction coefficient is much higher, and it continuously increases during the tests reaching a value of about 0.6 after 25 minutes. Almost the same value of the steady-state friction coefficient, i.e., 0.6, was found during the PoD tests conducted using with traditional gray cast iron sliding against the same friction material [31].

### 3.3 Evolution of surface roughness and wear damage

In Table 1, the initial surface roughness,  $R_a$ , and the skewness,  $R_{sk}$ , of the unworn coatings are listed. These parameters were also measured at the end of the interrupted as well as the continuous tests. The results are listed in Table 5, and plotted in Fig. 5.

Disc	$R_a$ at the end of the interrupted test	$R_{sk}$ at the end of the interrupted test	$R_a$ at the end of the continuous test	$R_{sk}$ at the end of the continuous test
WC-CoCr As sprayed	2.0	-0.1	1.6	-0.2
Cr <sub>3</sub> C <sub>2</sub> -NiCr As sprayed	3.0	-0.2	2.9	-0.6
WC-CoCr Polished	0.9	-1.8	0.6	-3.0
Cr <sub>3</sub> C <sub>2</sub> -NiCr Polished	0.9	-2.8	0.4	-4.0

Table 5:  $R_a$  and  $R_{sk}$  surface parameters measured after the interrupted and continuous tests.

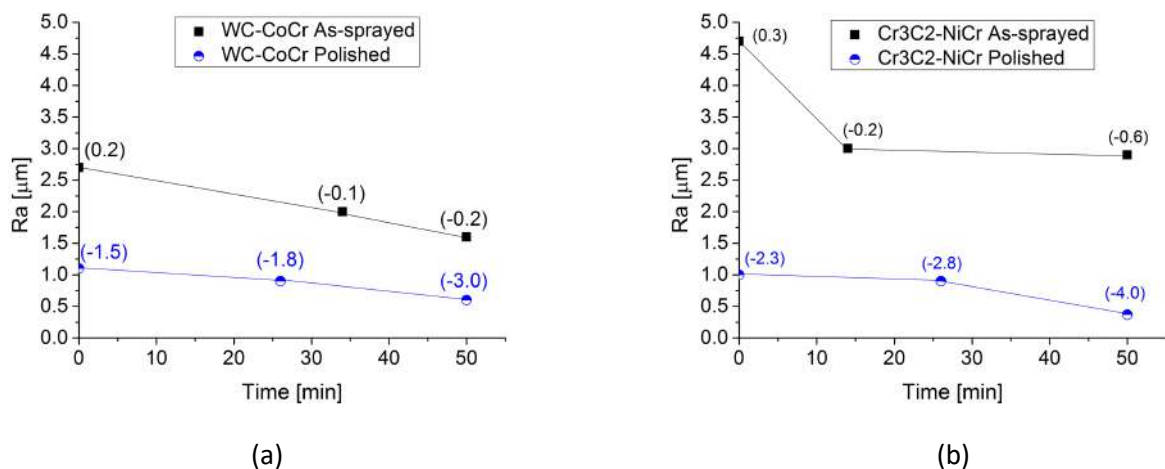


Fig. 5 Evolution of surface average roughness and, among brackets, roughness skewness parameter during PoD wear tests. Two sets of data are plotted: *interrupted* (a) and *continuous* (b) tests.

Fig. 5 clearly shows the progressive decrease in the average surface roughness and in the skewness as the sliding proceeds, for both the as-sprayed and the polished coatings. The controlled polishing procedure led to lower  $R_a$ -values and, most importantly, to a more negatively skewed surface profile that further decreased during sliding. The lowest skewness values were achieved with the polished discs. This is in agreement with the fact that more negative values of roughness skewness correspond to wider load bearing regions and to a more uniform contact with respect the as-sprayed coatings.

The worn surface of friction materials is typically characterized by the presence of friction layers, made by primary and secondary plateaus [3-9]. Figure 6 shows such plateaus observed on the pin surfaces after sliding against the  $\text{Cr}_3\text{C}_2\text{-NiCr}$  coated discs. The micrographs refer to the pins used both for the interrupted and the continuous tests. The letter (a) indicates a typical primary plateau, whereas with the letter (b) a typical secondary plateau is indicated. The EDXS analysis showed that primary plateaus are constituted by steel fibers, and that the secondary plateaus contain all the main ingredients of the friction material, with only a minor contribution from the disc coating.

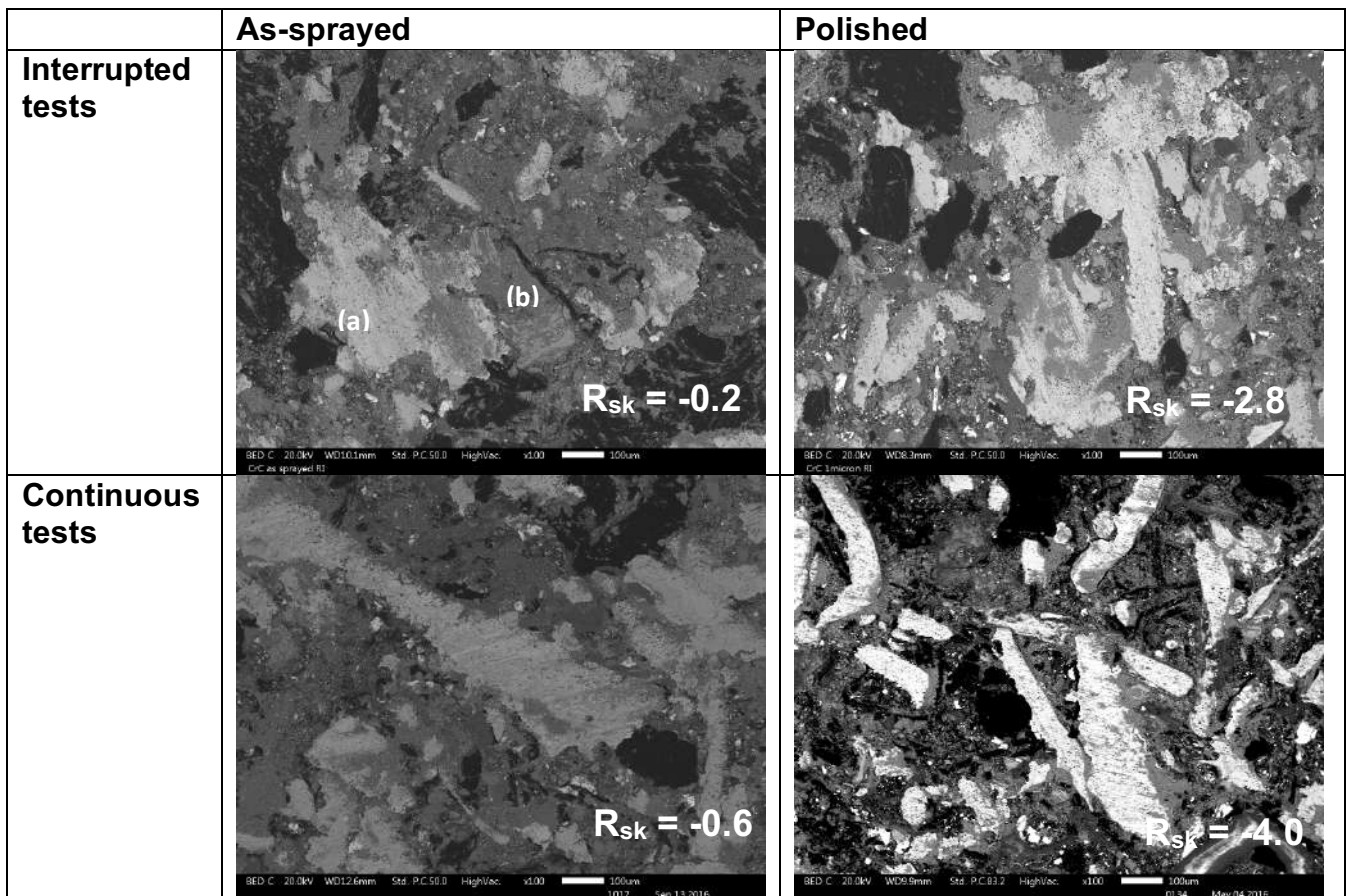


Fig. 6: SEM images of the worn surfaces of the pins after sliding against the  $\text{Cr}_3\text{C}_2\text{-NiCr}$  coatings in the as-sprayed and polished conditions, and in the case of the interrupted and continuous tests. The values of the relevant coating skewness,  $R_{sk}$ , are indicated (see also Table 5).

The general view of the wear tracks on the coated disc, tested both in the as-sprayed and polished conditions, are shown in Fig. 7. The wear tracks exhibit a uniform surface topography, indicating the occurrence of a homogeneous wearing out process.

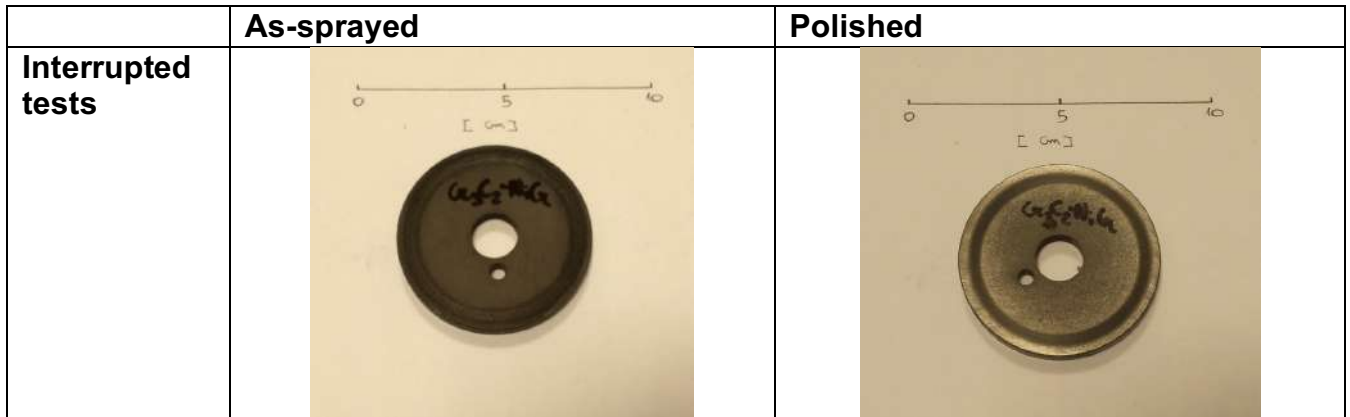


Fig. 7: General view of the wear tracks on the  $\text{Cr}_3\text{C}_2\text{-NiCr}$  coated discs in the as sprayed and polished conditions, after the interrupted tests.

Fig. 8 shows the SEM micrographs of the wear tracks on the coated discs. As already observed [16], the wear debris coming from the wear of the pins accumulated and compacted into the unpolished “valleys” of the polished coatings. The amount of material transferred from the pin onto the disc surface increases with its roughness and the micrographs of as-sprayed coatings clearly show this trend.

In order to confirm that during the sliding contact the coatings did not wear, EDXS elemental analyses and maps were acquired on the wear tracks of the polished coatings continuously tested. Since the polishing procedure leads to a decrease in the coating thicknesses only the polished coatings were analyzed. The results of these analyses are shown in Fig. 9 and Table 6.

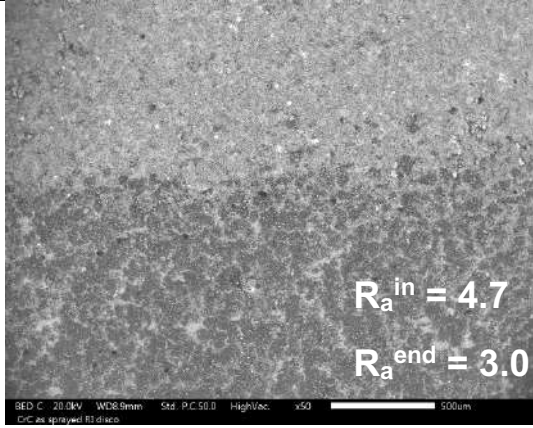
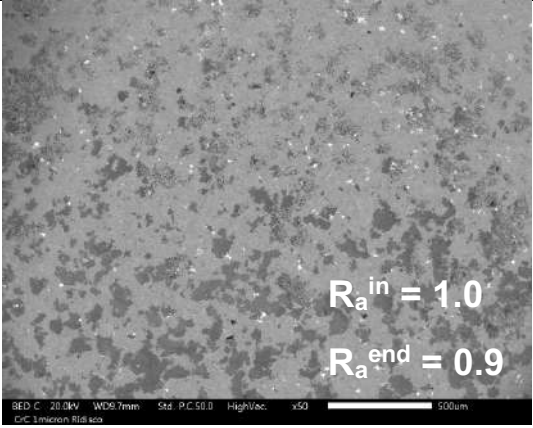
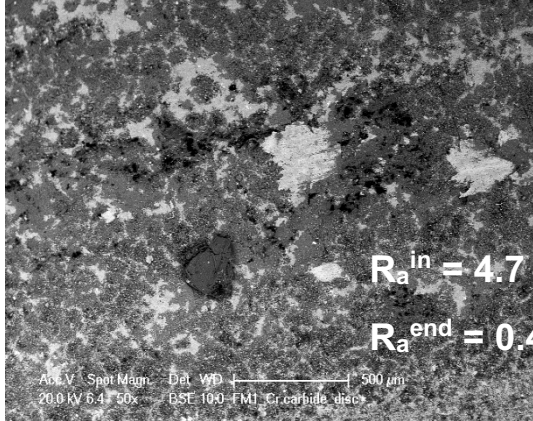
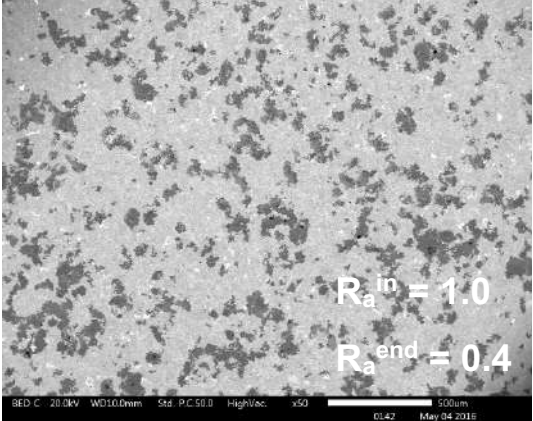
	As-sprayed	Polished
Interrupted tests	 <p><math>R_a^{in} = 4.7</math> <math>R_a^{end} = 3.0</math></p> <p>BED C 20.0kV WD8.9mm Std. P.C.50.0 HighVac. x50 500um CrC as sprayed R1 disc</p>	 <p><math>R_a^{in} = 1.0</math> <math>R_a^{end} = 0.9</math></p> <p>BED C 20.0kV WD9.7mm Std. P.C.50.0 HighVac. x50 500um CrC 1 micron R18 sco</p>
Continuous tests	 <p><math>R_a^{in} = 4.7</math> <math>R_a^{end} = 0.4</math></p> <p>ACL V Spot Magn Det WD 500um 20.0kV 6.4x50x BST 100-FM1 Cr carbide disc</p>	 <p><math>R_a^{in} = 1.0</math> <math>R_a^{end} = 0.4</math></p> <p>BED C 20.0kV WD10.0mm Std. P.C.50.0 HighVac. x50 500um 0142 May 04 2011E</p>

Fig.8: SEM images of the wear tracks on the disc surfaces after run-in the  $Cr_3C_2-NiCr$  coating in the as-sprayed and polished condition, after the interrupted and continuous test. The roughnesses refer to the average surface roughness,  $R_a$ , detected before and after the PoD tests.

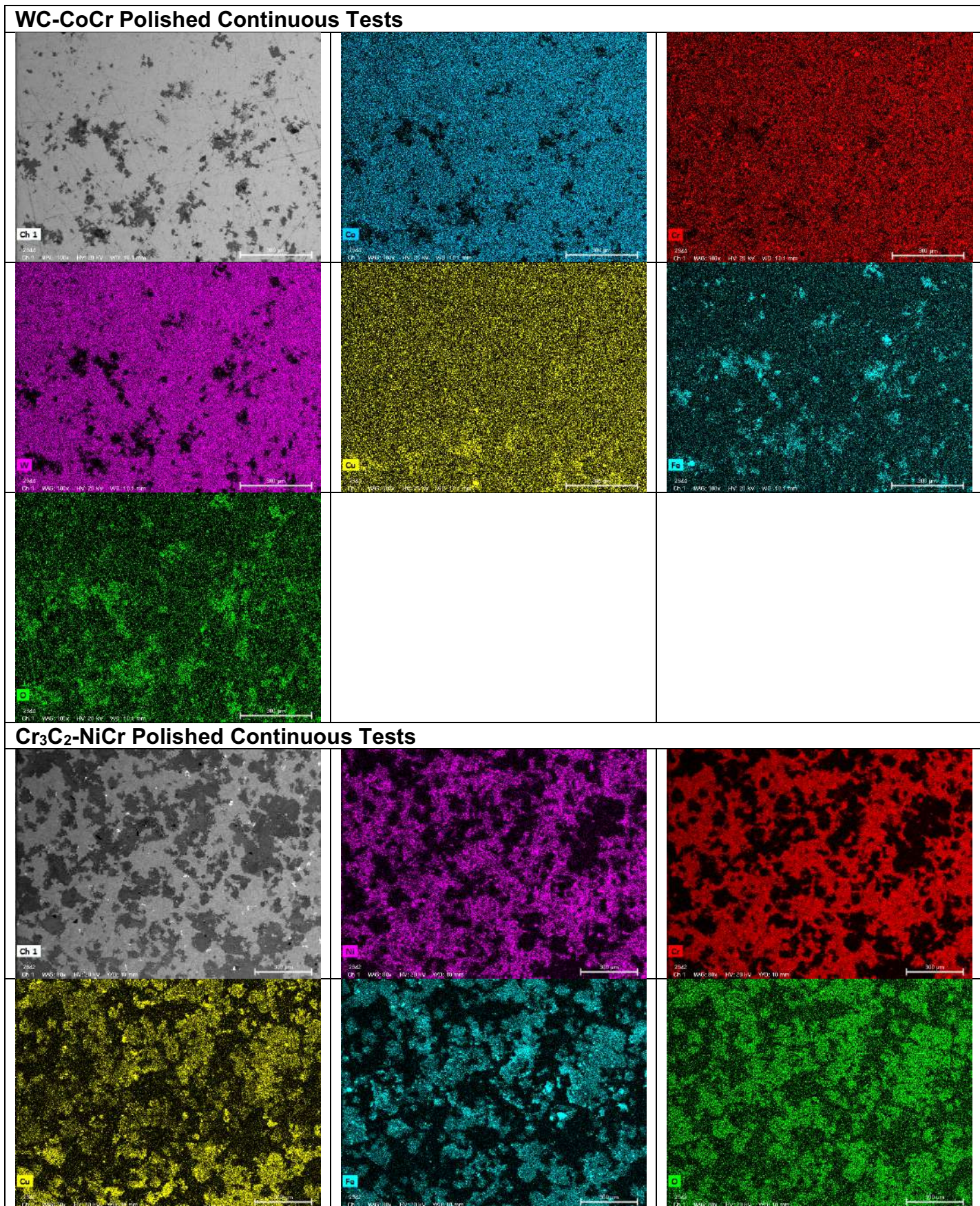


Fig. 9: EDXS elemental maps for the polished coatings continuously tested.

The results of the EDXS quantitative analysis are listed in Table 6.

Element	WC-CoCr [wt. %]	Cr <sub>3</sub> C <sub>2</sub> -NiCr [wt. %]
W	81.7	-
Cr	3.6	59.9
Co	9.7	-
Ni	-	20.3
Cu	0.8	7.6
Fe	1.4	7.1
O	2.8	5.1

Table 6: EDXS quantitative analysis of the polished coatings continuously tested.

## 4 Discussion

### 4.1 Wear behavior

In general, the stability and the extension of the secondary plateaus, resulting from the compaction of the wear debris against the reinforcing metal fibers, are strongly related to the surface topography of the disc counterface [16,33]. In a previous investigation [16], we observed that the asperities of the hard as-sprayed coatings tend to induce severe abrasive wear of the friction material and correspondingly to reduce the friction coefficient. After polishing, owing to the reduction in the initial roughness, the abrasive effect exerted by the asperities decreases, leading to a mild wear of the friction material and to a higher friction coefficient [31]. In the present study, we extend the former investigation [31] to the running-in stage of the PoD tests.

As shown by Figure 8, in the as-sprayed coatings the high initial roughness induces a significant transfer phenomenon that occurs from the beginning of the tests. This explains the high initial wear rates of the as-sprayed coatings, as shown by Figure 1a, and evidenced by the  $A_1$ -values listed in Table 4. In Figure 10 the almost linear relationship between the  $A_1$ -values and the initial roughness, expressed by the  $R_a$ -values, is highlighted. As already mentioned,  $A_1$  is an indicator of the wear rate during the first minutes of sliding contact; higher values of  $A_1$  are related to higher initial wear rates of the friction material.

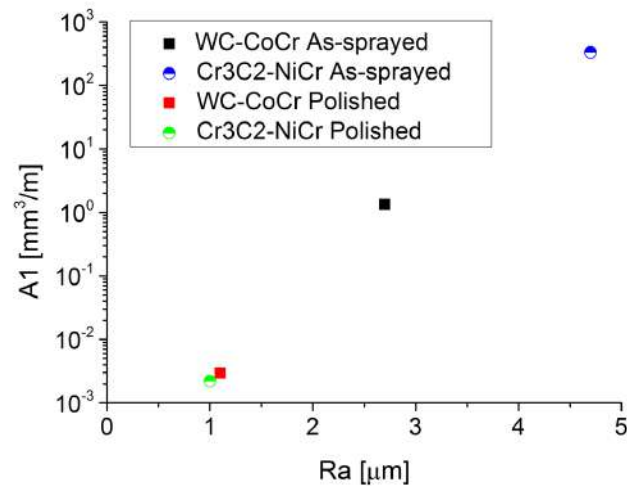


Fig. 10:  $A_1$  as a function of the initial roughness ( $R_a$ ) of the discs.

As can be noted from the SEM observations of the pin worn surfaces (Fig. 6), the extension of the friction layer decreases as the surface skewness becomes more negative. This phenomenon is strictly related to the increase in the load-bearing area that induces a lowering in the abrasive contribution of the asperities initially present on the unpolished coating surface. Upon reducing the wearing out of the friction material, the amount of wear debris decreases, leading to the formation of more compacted and adherent secondary plateaus. The same mechanism is valid for the transfer layer built up on the disc surfaces; the wear debris accumulated in the unpolished valleys of the coatings are more compacted in the case of low skewness values. The EDXS elemental maps in Fig. 9 clearly show the accumulation and the compaction of the wear debris inside the unpolished valleys of the coatings. Furthermore, the joint presence of copper and iron within the same areas and in similar ratios for the two coatings (see Table 6) is a further proof that the detected iron comes from the friction material (pin). As a further indication, the EDXS quantitative analysis revealed a comparatively low amount of iron on the wear tracks. This low amount can be ascribed to the transfer from the pin materials rather than to the exposition of the gray cast iron substrate.

Fig. 11 shows the relationship between the steady-state wear rate of the pins ( $W_\infty$ ) and the skewness at the end of the interrupted running-in tests. Coherently with the above results, the increase of the load-bearing area, due to the decrease in the skewness, leads to a more efficient compaction of the wear debris inside the unpolished valleys of the coatings and thereby to lower wear rates.

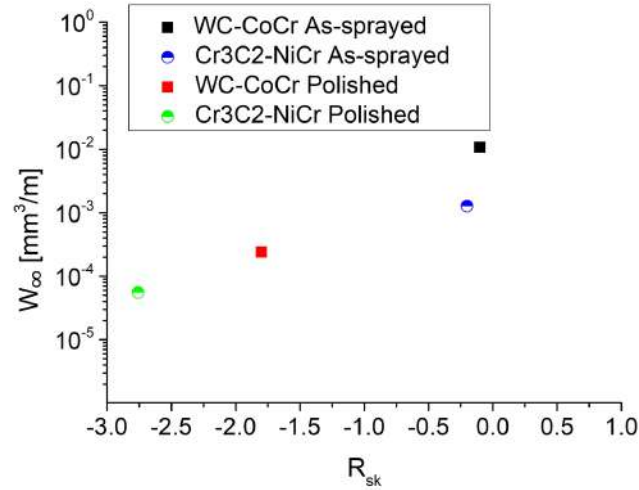


Fig. 11: Steady state wear rate of the pin ( $W_{\infty}$ ) as a function of the skewness at the end of the interrupted tests.

## 5.2 Friction Behavior

The friction coefficient of two mating surfaces under sliding conditions is given by two different contributions [34]:

$$\mu = \mu_{abr} + \mu_{ad}$$

where  $\mu_{abr}$  and  $\mu_{ad}$  are the abrasive and the adhesive contributions respectively. Using the Rabinowicz's model [35], it turns out that the abrasive contribution ( $\mu_{abr}$ ) due to the surface roughness generally does not exceed 0.2. This explains why low friction coefficients were exhibited by the as-sprayed coatings. In fact in this case, the friction coefficient is mainly determined by the abrasive interaction of the hard asperities. Furthermore, the trend of the friction coefficient during the continuous tests of the as-sprayed coatings, does not show the rise typically exhibited by the polished coatings (see Fig. 4(c) and (d)). Indeed, the abrasive contribution of the asperities determines the friction coefficient also after long sliding distances.

After reducing the surface roughness ( $R_a$ ) and skewness ( $R_{sk}$ ) by means of a controlled mechanical polishing treatment, the friction coefficient displayed an increasing trend during the continuous tests (Fig. 4(d)). During the interrupted tests the values of the friction coefficient of the polished discs were higher than the values detected for the as-sprayed coatings. However, the increasing trend observed in the continuous tests was no detected any longer (Fig. 4(a)). The general increase in the friction coefficient measured with the polished coatings can be explained by the rise of the adhesive contribution ( $\mu_{ad}$ ) associated with the increase in the load-bearing area. The increase in the adhesive contribution is particularly evident during the continuous tests. Rabinowicz [35] related the strength of the adhesive forces to the degree of contaminants on the sliding surfaces; the interruptions of the sliding tests lead to a higher degree of contamination, due to air humidity and pollutants, whose lubricating action hinders the rise of the friction coefficient to the same value as in the continuous test regime.



## 6 Conclusions

The running-in wear behavior of a commercial friction material (pin) dry sliding against two types of HVOF coatings was evaluated. The surface parameters, i.e., the roughness,  $R_a$ , and the surface asperity skewness,  $R_{sk}$ , were related to the wear behavior of the coatings. The main findings can be summarized as follows:

- the hard asperities of the as-sprayed coatings induce a severe abrasive wear of the pin material during PoD tests, with a relevant transfer of friction material onto the disc surfaces;
- the decrease in the surface roughness and skewness, achieved with a mechanical polishing treatment, reduces the abrasive contribution of the asperities leading to lower wear rates of the pins and to a lower material transfer on the disc surfaces;
- the initial wear rate of the friction material ( $A_1$ ) is significantly reduced by applying the polishing treatment, resulting in shorter running-in stage, more efficient in creating the steady state contact conditions between the pin and the disc;
- the disc surface polishing reduces the steady state wear of the friction material ( $W_\infty$ ) by two order of magnitude with respect the tests performed on the as-sprayed coatings;
- the polished coatings reduce the total wear rate also with respect to wear rate obtained in PoD tests with the same friction material sliding against a (uncoated) cast iron disc.
- the results show that starting the running-in with a negatively-skewed coating surface is fundamental to achieve the best frictional performances.
- the spontaneous surface modifications originating from wear phenomena during PoD testing are not as efficient as the controlled mechanical polishing in reducing the skewness and in improving the performances of the as-sprayed coated discs.

Ongoing research is focusing on the optimization of the composition of the coatings and of the friction material with the twofold aim: improving brake performances; reducing the emission of particulate matter during the braking action, in order to comply with the international regulations and standard. In this regard, the low wear rate of the pin-disc system looks promising indeed, since clear indications on the critical parameters could be inferred. Starting from these experimental results further dyno-bench tests need to be carried out to evaluate the performances of real components.

## Acknowledgments

The research leading to these results received funding from the European Union's Horizon 2020 Research and Innovation Action programme under the grant agreement No. 636592 (LOWBRASYS project). The Authors would also like to thank Flame Spray (Roncello, Italy), partner in the mentioned Project, for the deposition of the coatings, and to our former master student Roberto Moratti for his help in the experimental testing during his thesis.

## References

- [1] J.F. Archard, Contact and rubbing of flat surfaces, *J. Appl. Phys.* 24 (8) (1953) 981-988.
- [2] P.J. Blau, E.P. Whitenton, A. Shapiro, Initial frictional behavior during the wear of steel, aluminum and poly(methyl methacrylate) on abrasives papers, *Wear* 124 (1988) 1-20.
- [3] M. Eriksson, S. Jacobson, Tribological surfaces of organic brake pads, *Tribol. Int.* 33 (2000) 817-827.
- [4] M. Eriksson, F. Bergman, S. Jacobson, On the nature of tribological contact in automotive brakes, *Wear* 252 (2002) 26-36.
- [5] M. Eriksson, F. Bergman, S. Jacobson, Surface characterisation of brake pads after running under silent and squealing conditions, *Wear* 232 (1999) 163-167.
- [6] P.C. Verma, L. Menapace, A. Bonfanti, R. Ciudin, S. Gialanella, G. Straffelini, Braking pad-disc system: Wear mechanisms and formation of wear fragments, *Wear* 322-323 (2015) 251-258.
- [7] M. G. Jacko, P. H. S. Tsang, S. K. Rhee, Wear debris compaction and friction film formation of polymer composites, *Wear* 133 (1989) 23-38.
- [8] J. Jiang, F. H. Stott, M. M. Stack, The role of triboparticulates in dry sliding wear, *Tribol. Int.* 31 (5) (1998) 245-256.
- [9] A. Wirth, D. Eggleston, R. Whitaker, A fundamental tribochemical study of the third body layer formed during automotive friction braking, *Wear* 179 (1994) 75-81.
- [10] R. Kumar, B. Prakash, A. Sethuramiah, A systematic methodology to characterise the running-in and steady-state wear process, *Wear* 252 (2002) 445-453.
- [11] M. Hanief, M.F. Wani, Effect of surface roughness on wear rate during running-in of En31-steel: Model and experimental validation, *Mater. Lett.* 176 (2016) 91-93.
- [12] W. Wang, P.L. Wong, Z. Zhang, Experimental study of the real time change in surface roughness during running-in for PEHL contacts, *Wear* 244 (2000) 140-146.
- [13] M. Hanief, M.F. Wani, Modeling and prediction of surface roughness for running-in wear using Gauss-Newton algorithm and ANN, *Appl. Surf. Sci.* 357 (2015) 1573-1577.
- [14] M. Zheng, A.H. Naeim, B. Walter, G. John, Break-in Liner Wear and Piston Ring Assembly Friction in a Spark-Ignited Engine, *Tribol. T.* 41 (4) (1998) 497-504.
- [15] E.W. Schneider, D.H. Blossfeld, M.A. Balnaves, Effect of Speed and Power Output on Piston Ring Wear in a Diesel Engine, SAE Paper n. 880672, SAE, Warrendale, PA, 1988.
- [16] M. Federici, C. Menapace, A. Moscatelli, S. Gialanella, Effect of roughness on the wear behavior of HVOF coatings dry sliding against friction material, *Wear* 369-369 (2016) 326-334.
- [17] A.J. Day, *Braking of road vehicles*, Elsevier (2014).
- [18] G. Straffelini, L. Maines, The relationship between wear of semimetallic friction materials and pearlitic cast iron in dry sliding, *Wear* 307 (2013) 75-80.

- [19] G.M. La Vecchia, F. Mor, G. Straffelini, D. Doni, "Microstructure and sliding wear behavior of thermal spray carbide coatings", *Int. J. of Powder Metall.* 35 (1999) 37-46.
- [20] F. Mor, G.M. La Vecchia, D. Stehle, "Caratterizzazione di riporti thermal spray ottenuti con sistema HVOF al variare dei parametri di processo", *La Met. It.* 88 (1996) 363-370.
- [21] M. Xie, S. Zhang, M. Li, Comparative investigation of HVOF sprayed carbide-based coatings, *Appl. Surf. Sci.* 273 (2013) 799-805.
- [22] T. Saharaoui, N.E. Fenineche, G. Montavon, C. Coddet, Structure and wear behaviour of HVOF sprayed  $\text{Cr}_3\text{C}_2\text{-NiCr}$  and  $\text{WC-Co}$  coatings, *Mater. Des.* 24 (2003) 309-313.
- [23] G. Bolelli, L.M. Berger, M. Bonetti, L. Lusvarghi, Comparative study of the dry sliding wear behaviour of HVOF-sprayed  $\text{WC-(W,Cr)}_2\text{C-Ni}$  and  $\text{WC-CoCr}$  hardmetal coatings, *Wear* 309 (2014) 96-111.
- [24] W. Zhang, L. Liu, M. Zhang, G. Huang, J. Liang, X. Li, L. Zhang, Comparison between  $\text{WC-10Co-4Cr}$  and  $\text{Cr}_3\text{C}_2\text{-25NiCr}$  coatings sprayed on H13 steel by HVOF, *Trans. Nonferrous Met. Soc. China* 25 (2015) 3700-3707.
- [25] A. Gosh, F. Sadeghi, A novel approach to model effects of surface roughness parameters on wear, *Wear* 338-339 (2015) 73-94.
- [26] M. Sedlaček, B. Podgonrnik, J. Vižintin, Correlation between standard roughness parameters skewness and kurtosis and tribological behavior of contact surfaces, *Tribol. Int.* 48 (2012) 102-112.
- [27] Y. Ao, Q. J. Wang, P. Chen, Simulating the worn surface in a wear process, *Wear* 252 (2002) 37-47.
- [28] S. Hu, N. Brunetiere, W. Huang, X. Liu, Y. Wang, Evolution of bi-gaussian parameters of silicon-carbide and carbon-graphite discs in dry sliding wear process, *Tribol. Int.* 112 (2017) 75-85.
- [29] R. Dante, *Handbook of friction materials and their application-1<sup>st</sup> Edition*, Woodhead Publishing (2015).
- [30] M. Federici, G. Straffelini, S. Gialanella, Pin-on-Disc Testing of Low-Metallic Friction Material Sliding Against HVOF Coated Cast Iron: Modelling of the Contact Temperature Evolution, *Tribol. Lett.* 65 (2017) 121.
- [31] M. Federici, C. Menapace, A. Moscatelli, S. Gialanella, G. Straffelini, Pin on disc study of a friction material dry sliding against HVOF coated discs at room temperature and 300°C, *Tribol. Int.* 115 (2017) 89-99.
- [32] G. Straffelini, P.C. Verma, I. Metinoz, R. Ciudin, G. Perricone, S. Gialanella, Wear behavior of a low metallic friction material dry sliding against a cast iron disc: role of the heat-treatment of the disc, *Wear* 348-349 (2016) 10-16.
- [33] W. Wang, P.L. Wong, Wear volume determination during running-in for PEHL contacts, *Tribol. Int.* 33 (2000) 501-506.
- [34] G. Straffelini, *Friction and Wear, Methodologies for Design and Control*, Springer International Publishing, Switzerland, 2015.

[35] E. Rabinowicz, Friction and wear of materials, 2nd ed., Wiley (1995).

## Figure Captions

Fig. 1: SEM micrograph of a friction material cross section with the indication of the main constituents.

Fig. 2: Wear volume of pins as a function of the sliding time for (a) discs in the as sprayed conditions and (b) discs with an average roughness of  $1\mu\text{m}$ , obtained by surface polishing. Please note the completely different range for the y-axes.

Fig.3: Wear rate of pins as a function of the sliding time for (a) discs in the as sprayed conditions and (b) discs with an average roughness of  $1\mu\text{m}$ . Data points are fitted by the continuous lines given by Eq.1 (see main text).

Fig. 4: (a, b) Average friction coefficient in the case of the interrupted tests; (c, d): plots of the friction coefficient evolution during the continuous tests.

Fig. 5 Surface roughness and skewness parameter at the beginning and at the end of the interrupted (a) and continuous (b) tests.

Fig. 6: SEM images of the worn surfaces of the pins after sliding against the  $\text{Cr}_3\text{C}_2\text{-NiCr}$  coatings in the as-sprayed and polished conditions, and in the case of the interrupted and continuous tests. The values of the relevant coating skewness,  $R_{sk}$ , are indicated (see also Table 4).

Fig. 7: General view of the wear tracks on the  $\text{Cr}_3\text{C}_2\text{-NiCr}$  coated discs in the as sprayed and polished conditions, after the interrupted tests.

Fig. 8: SEM images of the wear tracks on the disc surfaces after run-in the  $\text{Cr}_3\text{C}_2\text{-NiCr}$  coating in the as-sprayed and polished condition, after the interrupted and continuous test.

Fig. 9: EDXS elemental maps for the polished WC-CoCr and  $\text{Cr}_3\text{C}_2\text{-NiCr}$  coatings continuously tested.

Fig. 10:  $A_1$  as a function of the initial roughness ( $R_a$ ) of the discs.

Fig. 11: Steady state wear rate of the pin ( $W_\infty$ ) as a function of the skewness at the end of the interrupted tests.